ELSEVIER

Catalysis Today 75 (2002) 401–405

CATALYSIS TODAY

www.elsevier.com/locate/cattod

Investigation of the oxygen storage process on ceria- and ceria–zirconia-supported catalysts

Sumeya Bedrane, Claude Descorme*, Daniel Duprez

Laboratoire de Catalyse en Chimie Organique (LACCO), UMR CNRS 6503, Poitiers University,
40, Avenue du Recteur Pineau, 86022 Poitiers Cedex, France

Abstract

A total of 10 noble metal (Rh, Pt, Pd, Ru and Ir) catalysts, either supported on CeO_2 or $Ce_{0.63}Zr_{0.37}O_2$, were prepared. Catalysts were fully characterized using XRD, N_2 adsorption at $-196\,^{\circ}C$, TEM and H_2 chemisorption. Oxygen storage processes were carefully investigated. The influence of temperature was checked and a key role of oxygen diffusion was further demonstrated. A review of the reactions involved in the CO transient oxidation reaction is finally proposed. © 2002 Elsevier Science B.V. All rights reserved.

Keywords: Ceria–zirconia; Oxygen storage capacity; Oxygen diffusion; Rh; Pt; Pd; Ru; Ir

1. Introduction

The progressive deterioration of the air quality is responsible for lots of public health and environmental problems. Since the automobile sector is a major contributor to atmospheric pollution, many studies dealt with the optimization of catalytic converters. In the case of three-way catalysts (TWC), ceria is being replaced by $Ce_xZr_{1-x}O_2$ mixed oxides with enlarged oxygen storage capacity (OSC) and higher thermal stability [1]. In the past decades, numerous papers reported on the investigation of structural and redox properties of these oxides [2,3]. However, only a few studies have been devoted to a better understanding of oxygen storage processes.

CeO_2 and $Ce_{0.63}Zr_{0.37}O_2$-supported catalysts are under study. Our attention was focused on the influence of the metal and the oxide structure on oxygen storage. The crucial role of the metal/oxide interface was also carefully analyzed.

2. Experimental

CeO_2 and $Ce_{0.63}Zr_{0.37}O_2$ oxides were directly supplied by Rhodia Electronics and Catalysis (La Rochelle, France) after calcination at 900 °C for 6 h. Catalysts were prepared by impregnation of the supports with the corresponding metal precursors ($Rh(NO_3)_3$, $Pt(NH_3)_4(OH)_2$, $Pd(NO_3)_3$, $Ru(NO)(NO_3)_3$ and $Ir[CH(COCH_3)_2]_3$). Metal loading was either 1 or 2 wt.%, depending on the molecular weight of the metal, in order to get the same metal atom percentage for all catalysts (around 100 μmol of metal atoms per gram of catalyst). Catalysts were dried at 120 °C for 24 h and pretreated for 4 h at 500 °C under flowing air or hydrogen ($30\,cm^3\,min^{-1}$). Catalysts final composition was checked by Elemental Analysis (CNRS, Service Central d'Analyse de Solaize, France).

---

* Corresponding author. Tel.: +33-5-49-45-39-97;
fax: +33-5-49-45-34-99.
E-mail address: claude.descorme@univ-poitiers.fr (C. Descorme).

PII: S0920-5861(02)00089-5

Materials structure was characterized by XRD using a Siemens D5005 diffractometer. Crystalline phases were identified by comparison with ICDD files. The average crystallite size was estimated from the Scherrer relation.

Surface areas were measured by N_2 adsorption at $-196\,^{\circ}C$ (single point method). Measurements were carried out in a Micromeritics Flowsorb II apparatus.

Metal dispersion was calculated from H_2 chemisorption experiments. All measurements were carried out under optimized conditions to prevent hydrogen spillover onto the support [4]. Additional transmission electron microscopy (TEM) direct observations were carried out in a CM 120 Philips microscope.

Finally, oxygen storage capacities were measured based on the method developed by Yao and Yu Yao [5]. Experiments were carried out in a pulse chromatographic system already described by Kacimi et al. [6]. A 5–10 mg sample is preheated under flowing He ($30\,cm^3\,min^{-1}$) before oxidation at the "reaction" temperature. In a first sequence, CO pulses are injected on the sample every 2 min up to full reduction of the sample and followed by O_2 pulses up to full re-oxidation. From this first step, the total amount of oxygen that can be stored in the oxide (OSCC) is accessed. Subsequently, the amount of oxygen immediately available (OSC) is measured by alternating CO and O_2 pulses every 2 min. OSC is expressed in micromoles of CO_2 produced per gram of catalyst.

3. Results and discussions

3.1. Materials characterization

The main characteristics of the materials under study are summarized in Table 1. Ceria–zirconia mixed oxide exhibits the highest thermal stability. In fact, after calcination at $900\,^{\circ}C$, $Ce_{0.63}Zr_{0.37}O_2$ surface area is about twice that of pure ceria (43 vs. $25\,m^2\,g^{-1}$). XRD characterizations confirmed the formation of a purely monophasic fluorite-type structure solid solution accompanied by a contraction of the unit cell upon substitution of Zr to Ce. Lattice parameter was calculated to be 5.4113 Å for CeO_2 and to decrease down to 5.3044 Å for $Ce_{0.63}Zr_{0.37}O_2$. Moreover, an average crystallite size of 66 Å was calculated for $Ce_{0.63}Zr_{0.37}O_2$ compared to 195 Å for CeO_2.

Table 1
Main structural characteristics of the solids under study

	CeO_2		$Ce_{0.63}Zr_{0.37}O_2$	
	S_{BET} ($m^2\,g^{-1}$)	Particle size (Å)	S_{BET} ($m^2\,g^{-1}$)	Particle size (Å)
Support	25	195[a]	43	66[a]
Rh	23	10[b]	38	15[b]
Pt	24	12[b]	42	12[b]
Pd	25	12[b]	38	15[b]
Ru	24	18[b]	37	13[b]
Ir	27	24[b]	36	32[b]

[a] Oxide crystallite size estimated from XRD measurements.

[b] Metal particle size calculated from H_2 chemisorption and TEM direct observations.

Looking at supported catalysts, metal dispersion—and metal particle size—was calculated from H_2 chemisorption measurements and TEM direct observations. These experiments evidenced a well-dispersed metallic phase, with particle sizes between 10 and 30 Å. A better dispersion is favored on CeO_2.

3.2. Oxygen storage capacities

Preliminary studies were carried out at $400\,^{\circ}C$ to check the influence of the metal on the OSC. At this temperature, OSC is increased by a factor of 4–9 in the presence of metal particles (153 and 363 $\mu mol\,CO_2\,g^{-1}$ catalyst for Pt/CeO_2 and Ir/CeO_2, respectively, vs. 41 $\mu mol\,CO_2\,g^{-1}$ for CeO_2). On both supports, iridium and ruthenium were shown to be the most effective to enlarge OSC.

Moreover, the influence of temperature on OSC was examined. From an earlier study carried out on ceria-supported Rh and Ir catalysts, it was demonstrated that OSC is restricted to the surface. On the opposite, bulk oxygen atoms do participate to the storage in the case of Rh and Ir ceria–zirconia-supported catalysts [7]. This study was extended and Figs. 1 and 2, respectively, show the evolution of the OSC as a function of temperature on ceria- and ceria–zirconia-supported Rh, Pt, Pd, Ru and Ir catalysts. At $500\,^{\circ}C$, based on the OSC expressed in micromoles CO_2 per gram of catalyst, the following sequence may be established: Ir > Ru > Rh > Pd > Pt. On ceria-based catalysts, oxygen storage is slightly activated (Fig. 1). At $200\,^{\circ}C$, OSC is restricted to the metal and/or to the particle vicinity. At higher temperature, OSC

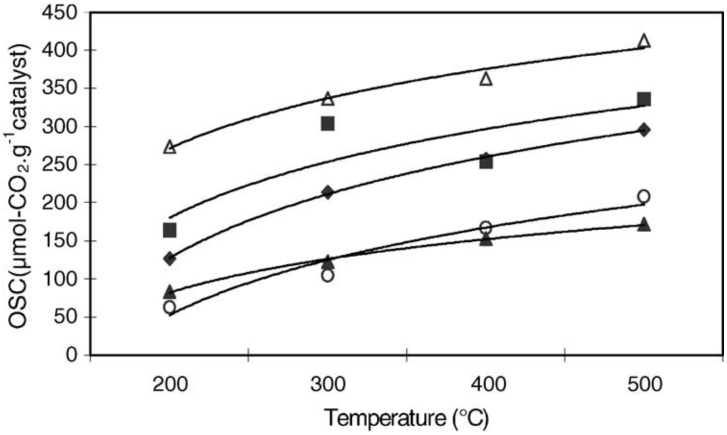

Fig. 1. Evolution of the OSC (expressed in µmol CO_2 g^{-1} catalyst) as a function of temperature (between 200 and 500 °C) on CeO_2-supported catalysts: (◆) Rh/CeO_2, (▲) Pt/CeO_2, (○) Pd/CeO_2, (■) Ru/CeO_2, (△) Ir/CeO_2.

increases slightly and reaches a maximum corresponding to full reduction of ceria surface (maximum OSC measured at 500 °C for Ir/CeO_2 is 413 µmol CO_2 g^{-1} catalyst vs. a theoretical value of 402 µmol CO_2 g^{-1} catalyst corresponding to full reduction of ceria surface plus reduction of IrO_2). On the opposite, on ceria–zirconia-supported catalysts, OSC widely increases between 200 and 400 °C (Fig. 2). Such a large increase in OSC is related to bulk reduction. Above 450 °C, oxygen storage is limited by bulk diffusion and no further increase is observed.

Whatever the metal, oxygen activation is fast. Metal particles are described as portholes for the subsequent migration of oxygen onto the support. Oxygen storage processes are then limited by diffusion either at the surface on ceria or in the bulk of mixed oxides. To go further in our interpretations, the number of oxygen layers involved in the storage process was calculated on the basis of the experimental OSC values and the theoretical number of reducible surface oxygen atoms as reported by Madier et al. [8]. Whatever the metal, figures summarized in

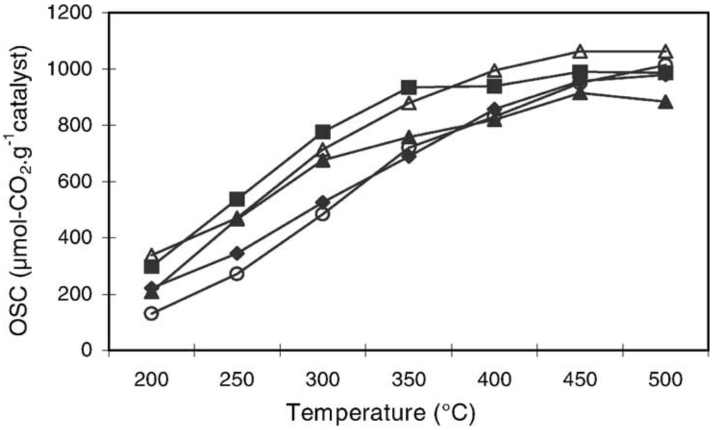

Fig. 2. Evolution of the OSC (expressed in µmol CO_2 g^{-1} catalyst) as a function of temperature (between 200 and 500 °C) on $Ce_{0.63}Zr_{0.37}O_2$-supported catalysts: (◆) Rh/$Ce_{0.63}Zr_{0.37}O_2$, (▲) Pt/$Ce_{0.63}Zr_{0.37}O_2$, (○) Pd/$Ce_{0.63}Zr_{0.37}O_2$, (■) Ru/$Ce_{0.63}Zr_{0.37}O_2$, (△) Ir/$Ce_{0.63}Zr_{0.37}O_2$.

Table 2
Contribution of metal particles to the total OSC and number of oxygen layers involved in the storage process

Catalyst	OSC_{exp}[a]	OSC_{metal}[b]	$O_{reducible}$[c]	NL[d]
Rh/Ce	296	115	136	1.3
Pt/Ce	172	84	136	0.6
Pd/Ce	208	91	136	0.9
Ru/Ce	336	196	136	1.0
Ir/Ce	413	266	136	1.1
Rh/CeZr	980	128	152	5.6
Pt/CeZr	883	95	152	5.2
Pd/CeZr	1015	109	152	6.0
Ru/CeZr	985	210	152	5.1
Ir/CeZr	1062	308	152	5.0

[a] Maximum OSC measured at 500 °C and expressed in micromoles of CO_2 formed per gram of catalyst.

[b] Number of O atoms necessary for a complete reduction of metal oxides (Rh_2O_3, PtO, PdO, RuO_2 and IrO_2) expressed in micromoles of O atoms per gram.

[c] Number of reducible oxygen atoms per oxygen layer [8].

[d] Number of oxygen layers involved in the storage process.

Table 2 clearly show that oxygen storage is restricted to the surface of ceria while bulk oxygen atoms are involved in the case of ceria–zirconia-supported catalysts.

In fact, earlier studies showed that oxygen mobility is fast on $Ce_{0.63}Zr_{0.37}O_2$ [9]. Upon CO pulses, bulk oxygen atoms may diffuse to the surface and further react with CO molecules. In the case of ceria, oxygen diffusion in the bulk is almost zero and the CO transient oxidation reaction stops after full reduction of the surface.

To go further into oxygen storage processes, possible reactions are listed below. Upon CO pulses, O atoms stored in the oxide diffuse and react with adsorbed CO molecules to form CO_2 (1). If all CO molecules would react with oxygen atoms, CO uptake and CO_2 production should be equal. However, in all cases, more CO is consumed compared to CO_2 formed. In fact, some CO may react with surface dioxygen species to form carbonates species left over the surface (2). Both dioxygen and carbonates species were evidenced by IR studies [10–14]. Additionally, two CO molecules may disproportionate to form CO_2 and a C deposit (3). Furthermore, CO may dissociate on an oxygen vacancy to form residual C and fill in the vacancy (4). Finally, CO may also react with surface hydroxyl groups to produce CO_2 and H_2 via the water–gas shift reaction (5):

$$CO + O_s \rightarrow CO_2 \quad (1)$$

$$CO + O_2^{2-} \rightarrow CO_3^{2-} \quad (2)$$

$$2CO \rightarrow C_s + CO_2 \quad (3)$$

$$CO + \square \rightarrow C_s + O_s \quad (4)$$

$$CO + OH \rightarrow CO_2 + \tfrac{1}{2}H_2 \quad (5)$$

Nevertheless, in the experiments herein presented, no H_2 formation is detected and the participation of the WGS reaction to the oxygen storage process may be ruled out. No CO_2 derives from the oxidation of CO involving surface OH groups.

Upon O_2 pulses, oxygen atoms dissociatively adsorbed on the metal particles migrate back to the oxide surface (6). The support is then re-oxidized. After oxygen pulses, CO_2 is also produced. In that case, CO_2 production corresponds to the reaction of oxygen with surface carbon deposits (7):

$$\tfrac{1}{2}O + \square \rightarrow O_s \quad (6)$$

$$O_2 + C_s \rightarrow CO_2 \quad (7)$$

Table 3
Oxygen and carbon mass balances

Catalyst	200 °C		400 °C	
	Carbon[a]	Oxygen[b]	Carbon[a]	Oxygen[b]
CeO_2	0	0	7	22
Rh/Ce	20	54	−10	−10
Pt/Ce	26	55	12	35
Pd/Ce	25	54	10	−9
Ru/Ce	29	100	30	15
Ir/Ce	4	60	26	−19
$Ce_{0.63}Zr_{0.37}O_2$	0	0	7	21
Rh/CeZr	56	138	7	−97
Pt/CeZr	52	127	52	−61
Pd/CeZr	24	145	43	48
Ru/CeZr	45	116	44	−12
Ir/CeZr	56	104	44	−106

[a] Expressed in micromoles of C atoms per gram of catalyst (a positive value indicates that C is left over the surface after CO transient oxidation reaction).

[b] Expressed in micromoles of O atoms per gram of catalyst (a positive value indicates that the sample is over-oxidized while a negative value would indicate that O is irreversibly lost by the solid).

Based on this set of reactions, a carbon and oxygen mass balance was systematically established (Table 3). Residual carbon was calculated from the difference between the CO uptake and the total CO_2 production. Residual oxygen corresponds to the difference between the total oxygen uptake (CO and O_2 uptake) and the total CO_2 production.

On bare oxides, residual oxygen and residual carbon are almost zero. Nevertheless, at 400 °C, $O_{residual}$ is about three times $C_{residual}$. As a result, one can conclude that some oxygen is stored on the support as carbonates. On the catalysts, two different trends are observed: (i) at low temperature, residual oxygen is high and the catalyst is virtually over-oxidized. Again, $O_{residual}$ is two or three times $C_{residual}$ and some oxygen atoms seem to be stored in the form of carbonates and carbonites surface species (CO_3^{2-} and CO_2^{2-}) [13,14], (ii) at high temperature, the oxygen mass balance is negative in most cases while less C deposit is evidenced. As a result, the support appears to be irreversibly reduced. In every case, the nature of the metal does not greatly influence these main features. Nevertheless, the formation of carbon deposits appeared to be favored on ceria–zirconia-supported catalysts.

4. Conclusions

OSC was shown to be widely enhanced by the presence of metal particles on the oxide surface. Iridium and ruthenium appeared as the most effective to enlarge the OSC among all tested metals. Moreover, investigations on the influence of temperature evidenced interesting features. On both supports, oxygen activation is fast, with metal particles acting as portholes for the subsequent migration and storage of oxygen on the support. OSC on ceria-based catalysts was shown to slightly vary with temperature. Maximum OSC corresponds to a full reduction of the surface. On the opposite, on ceria–zirconia-supported catalysts, OSC widely increases with temperature. Bulk reduction is then responsible for such variations and oxygen diffusion in the bulk controls the process. Furthermore, looking at carbon and oxygen mass balances, one may note that oxygen could very partly be stored in the form of carbonates species. Catalysts appeared to be over-oxidized at low temperature while irreversibly reduced at high temperature. Finally, the reactions involved in the oxygen storage processes are proposed to interpret these features.

References

[1] G. Vlaic, R. Di Monte, P. Fornasiero, E. Fonda, J. Kaspar, M. Graziani, Stud. Surf. Sci. Catal. 116 (1998) 185.
[2] P. Fornasiero, G. Balducci, R. Di Monte, J. Kaspar, V. Sergo, G. Gubitosa, A. Ferrero, M. Graziani, J. Catal. 164 (1996) 173.
[3] P. Fornasiero, R. Di Monte, G. Ranga Rao, J. Kaspar, S. Meriani, A. Trovarelli, M. Graziani, J. Catal. 151 (1995) 168.
[4] Y. Madier, Ph.D. Thesis, Poitiers University, 1999.
[5] H.C. Yao, Y.F. Yu Yao, J. Catal. 86 (1984) 254.
[6] S. Kacimi, J. Barbier Jr., J.R. Taha, D. Duprez, Catal. Lett. 22 (1993) 343.
[7] S. Bedrane, C. Descorme, D. Duprez, Stud. Surf. Sci. Catal. 138 (2001) 125.
[8] Y. Madier, C. Descorme, A.M. Le Govic, D. Duprez, J. Phys. Chem. B 103 (1999) 10999.
[9] C. Descorme, Y. Madier, D. Duprez, T. Birchem, Stud. Surf. Sci. Catal. 130 (2000) 347.
[10] C. Li, K. Maruya, T. Onishi, J. Am. Chem. Soc. 111 (1989) 7683.
[11] C. Li, K. Domen, K. Maruya, T. Onishi, J. Catal. 123 (1990) 436.
[12] C. Descorme, Y. Madier, D. Duprez, J. Catal. 196 (2000) 167.
[13] C. Li, Y. Sakata, T. Arai, K. Domen, K. Maruya, T. Onishi, J. Chem. Soc., Faraday Trans. 1 85 (4) (1989).
[14] C. Binet, A. Badri, M. Boutonnet-Kizling, J.-C. Lavalley, J. Chem. Soc., Faraday Trans. 90 (7) (1994) 1023.